Advances in Electro-optic Polymer Waveguide Devices

K-JIST
교 수 김 장 주

ADVANCES IN ELECTRO-OPTIC POLYMER WAVEGUIDE DEVICES

J.-J. KIM*[a], W.-Y. HWANG[b], H. PARK[b], M.-C. OH[b], S.-Y. Shin[c]
a K-JIST, Kwangsan, Kwangju 506-712 Korea
b ETRI, P.O. Box 106, Yusong, Taejon, 305-600 Korea
c KAIST, Yusong, Taejon, Korea

Abstract Recent advances in electro-optic polymer waveguide devices are summarized. Device technology especially to fabricate modulators is mature now for practical use. Combination with high performance materials will guarantee the success of the devices. Along with the modulators, novel switches and various polarization control devices have been actively pursued, resulting in high performance devices. Those devices are utilizing the unique properties of EO poled polymers such as the flexibility of the fabrication process and the controllability optic axis, which are not possible in other materials. A method to tune the specification of waveguide devices after the completion of the device fabrication is also introduced, which is called post-photobleaching technique. This is a valuable technique to increase the fabrication yield.

INTRODUCTION

Very high hyperpolarizability found in some molecules about two decades ago attracted large attention in the hope to get efficient blue light by the second harmonic generation. No efficient blue emitting material existed at the time. Advantage of polymers for high-speed waveguide devices was also identified at the early stage of the research on polymer devices, which has been proved recently by the demonstration of 110 GHz modulator[1].

Soon after the high hope, however, many problems have been disclosed one by one. The first and important one was to develop methods to orient nonlinear optical molecules and maintain the orientation at elevated temperature, leading to the thermal stability issue. Various methods have been developed to improve the thermal stability since then. These include the side chain polymers with high glass transition temperature, cross-linking system and dye doped in highly stable polymers like polyimide. Effort to increase the nonlinearity has also been continued to get large advances in recent years[2]. Electro-optic coefficient over 55 pm/V was reported at 1.3 μm without absorption tail at the wavelength[3]. Some of the problems have been identified with the progress of the device research. They include the poling induced optical loss[4], photochemical stability[5], and dc bias stability[6]. It is now believed that most of the problems are exposed and the origins behind them are identified.

In this paper, status of EO modulators and switches will be summarized and their performance will be compared to the requirements for communication application. Novel polarization control devices will be described, which utilize the controllability of optic axis in poled polymers. Based on this, we will discuss the prospect of the devices. Post-photobleaching technique will also be introduced, which is useful to tune the device characteristics after the completion of the device fabrication.

STATUS OF EO POLYMER MODULATORS

Nonlinear optical polymer has advantages to realize high-speed EO waveguide devices. The advantages come from the fact that most polymers have low dielectric constant with low dispersion from dc to optical frequency, which results in the small velocity mismatch between microwave and optical signals in traveling wave type devices. Theoretical limit of bandwidth-electrode length product of a traveling wave type EO modulator due to velocity mismatch can be expressed as follows.

$$f \cdot L = \frac{c}{4\left|n_{eff} - \sqrt{\varepsilon_{eff}}\right|} \quad (1)$$

where f is the modulation frequency, L the interaction length, c the speed of light, n_{eff} the effective index of refraction, ε_{eff} the effective dielectric constant. Since the difference in velocity between light wave and microwave for most polymers is small, this limit can be over 120 GHz·cm. On the contrary, it is less than 20 GHz·cm for $LiNbO_3$ or GaAs.

The research on EO polymer based high speed modulator started in the early 1990's, demonstrating the modulation bandwidth over 110 GHz recently[1]. The progress of the research during the last several years is summarized in Table 1. The results clearly show that EO polymers are superior to other materials for high-speed devices.

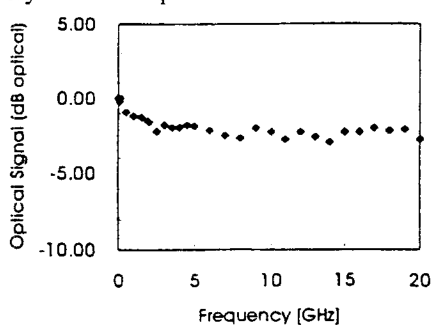

Fig. 1. Frequency response of the optical modulation measurement of traveling wave type electro-optic polymer modulator.

We have also fabricated EO modulators with the 3dB bandwidth the 20 GHz. The modulation characteristics of the device are shown in Fig. 1. Thermal stability of the devices has been improved much during the last decade by employing the thermoset or thermally stable polymers[10-15]. A device possessing the thermal stability to 350°C was reported by using stable chromophores incorporated in polyimide[13]. The nonlinearity of the material is comparable to DR1 based side chain polymers.

At the same time, effort to decrease the modulation voltage has been made by the improvement in material nonlinearity and the optimization of the device structure[17-19]. We have recently obtained a halfwave voltage of 3.7 V with a 1.5 cm long modulation electrode at the wavelength of 1.3 μm, which corresponds to the halfwave voltage-modulation length product of 5.5 V·cm[20]. The value is the lowest ever reported until now, and indicates that the modulation voltage lower than 3 V is readily achievable if a longer modulation electrode than 2 cm is employed. The low value of halfwave voltage was obtained by optimizing the device structure and the electrical properties of the cladding material. By the way we could improve the poling efficiency significantly resulting in high EO coefficient and low modulation voltage even with the same material. The modulation extinction was over 20 dB and the propagation loss was 1 dB/cm at the wavelength of 1.3 μm, promising the total insertion loss lower than 10 dB. The modulation characteristics of the device are shown in Fig.2. The performance is nearly satisfying the requirements for high speed telecommunication applications.

Recently, the issue of the dc bias stability was raised for the polymer EO modulator. Mach-Zehnder intensity modulators may require the adjustment of the retardation by a dc electric field in the EO layer, e.g., to operate in the linear region. However, the required voltage may change with time. This phenomenon is called the dc

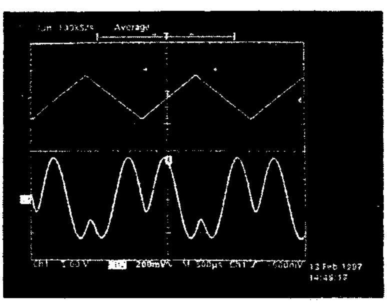

(a)

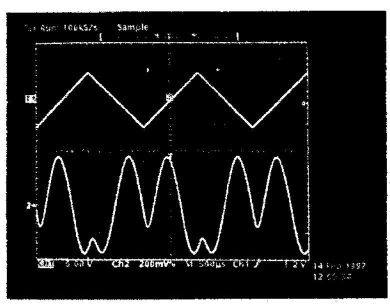

(b)

Fig. 2. Modulation characteristics of a low modulation voltage electro-optic modulator for the triangular electrical input of 500 Hz: (a) at the wavelength of 1.3 μm with peak-to peak voltage (Vp-p) of 8V and (b) at the wavelength of 1.55 μm with Vp-p=10 V.

bias drift. It was recently shown that the dc drift phenomenon can be explained by an equivalent circuit model of the resistance and capacitance of the consisting layers. The model showed that it is originated from the difference of the relaxation times of the guiding and the cladding layers[6]. In order for the dc bias to be at least traceable, the relaxation time (dielectric constant/conductivity) of the guiding layer must be smaller than the cladding layer, which is called 'the condition of the electrical compatibility' between the guiding and the cladding materials[21]. This condition gives another restriction in selecting a cladding layer. We have proved that the dc drift can be made traceable by properly selecting a cladding material based on the analysis[6].

The above summary indicates that it would not be very far from now to realize practical EO polymer modulators if the matured device technology is combined with advanced materials. Some companies are fabricating packaged devices and doing field test for the applications to communication[15].

Table 1. Progress in EO polymer intensity modulator

Band-width	Vπ (V), L (mm)	Insertion loss (dB)	Extinction ratio (dB)	Thermal stability	Material	Year	Ref.
20 GHz	9V, 17mm	-	>20	-	DANS	1991	8
40 GHz	10V, 12mm	-	>20	-	P2ANS	1992	9
20 GHz	19V, 16mm	12 dB	12	75 °C	NEHABR	1993	10
40 GHz	-	13 dB	13	60 °C	PUR-DR19	1995	11
>1 GHz	16V, 15mm	>10 dB	10	60 °C	3RDCVXY	1995	12
50 GHz	5V, 26mm	-	-	375 °C	DCM in PI	1995	13
60 GHz	-	-	-	60 °C	PUR-DR19	1995	14
18 GHz	11V,	13-15	-	60 °C	PUR-DR19	1996	15
113 GHz	-	-	-	60 °C	PUR-DR19	1997	1
4 GHz	9V, 15mm	31	13.2	-	DANS	1997	16

SWITCHES

Electro-optic 2x2 switches based on waveguide structures are one of the elementary components for optical signal processing. Switching principles such as interference, total internal reflection, and mode evolution have been applied to realize the devices using the various materials such as $LiNbO_3$, GaAs, and InP. However, EO polymers switches have not been actively investigated up to now. There are only a few reports on the device based on the directional couplers[22,23] and the balanced MZ interferometer incorporating 3-dB couplers[24]. However, these devices have some drawbacks.

Directional coupler switches require $\sqrt{3}$ times higher switching voltage than the interferometric switches. Also it is not easy to adjust the coupling states to crossover or 3-dB coupling states.

Recently, we have reported a 2x2 EO polymer switch, which consists of a pair of asymmetric Y-junctions and the MZ interferometer[25]. A schematic diagram of the device structure is shown in Fig. 3. The device exploits the mode evolution and the interference effects simultaneously. Therefore it does not require precise control of the refractive index and the waveguide dimensions. The required switching voltage is lower than that of the DC and the digital switches. One difficulty of realizing the device comes from the fabrication of the asymmetric Y-junctions. Good switching extinction requires a small branching angle less than 1° to activate the adiabatic mode evolution. The photobleaching technique in EO polymers is especially suitable to form very fine channels, because it is the room temperature process and does not contain any wet process. Therefore, we can expect very smooth asymmetric Y junctions for the adiabatic mode evolution, which ensures low crosstalk with good reproducibility.

The asymmetric Y junction consists of the mode evolution region and the two mode region. Mode evolution in the asymmetric Y junction takes place if the branching angle θ_1 is small enough to satisfy the condition of $\theta 1 << \Delta\beta/\gamma$[26]. Here $\Delta\beta$ is the difference between the propagation constants of the two branched waveguide and γ is the average of their transverse propagation constant in the cladding region. The fundamental even mode (the zeroth mode) or the first higher order odd mode (the first mode) could be excited in the two mode region depending on the port through which the light is launched. The odd-mode is excited if the light is launched through the narrow port 1 and the even mode if through the wide port 2. That is because the mode evolution is directed to a local guiding mode with closer propagation constant of the coming light.

The evolved mode (even or odd mode) is split into and propagates through the two arms of the MZ interferometer. The output lights from the two arms are combined in the output two mode region. If there is no phase difference between the lights from the two arms, the mode evolved in the input junction is reconstructed in the output junction. Because of the mode evolution effect in the output asymmetric Y junction, the

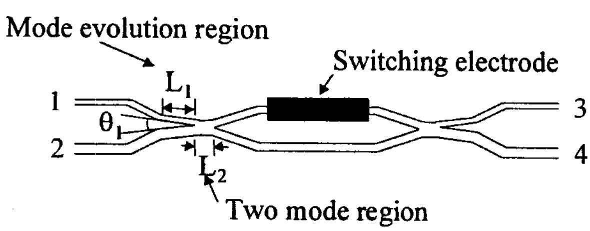

Fig. 3. Schematic diagram of the designed 2x2 switch

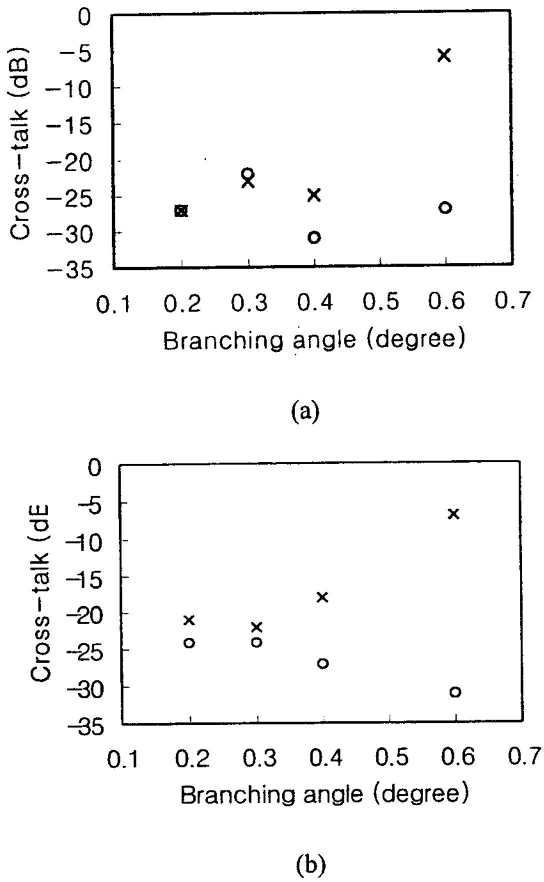

Fig. 4 Crosstalks for different branching angles of the crossover (x) and the straight-through (o) states when light is coupled through (a) the port 1 and (b) port 2 in Fig. 3. .

switch is in the straight-through state. On the contrary, if the light in one arm experiences the phase difference of π, the mode evolved in the input junction is now switched from the even to the odd or from the odd to the even in the output junction region. The device is now switched to the cross over state.

Optimum structure of the device was designed using the two dimensional beam propagation method and fabricated using a DANS based EO polymer. Details of the dimensions and the fabrication procedure are described elsewhere[25]. The switches showed excellent switching characteristics with the crosstalk better than –22 dB for the branching angles of 0.2° and 0.3° as shown in Fig. 4. The crosstalk becomes worse as the branching angle increases from them. The switching voltage was 15 V and the insertion loss was 9-10 dB at 1.3 μm when coupled by lens. These characteristics indicate that EO polymers are eligible to achieve high performance switches.

NOBLE PROPERTIES OF EO POLYMERS IN WAVEGUIDE DEVICES

Along with the high speed possibility, EO polymers have a variety of advantages for waveguide applications over inorganic crystalline materials. The fact that the device is fabricated by stacking layer by layer can be used to fabricate multiple stack EO modulators or a vertically coupled switch. Photobleaching technique which is routinely employed to form channel waveguides can be utilized to perform *in situ* tuning of the device specification after the completion of the device fabrication, which is so called *post-photobleaching technique*. Another noble properties of EO poled polymers include the controllability of the optic axis and the magnitude of the birefringence induced by the poling process. These properties can be exploited to design and fabricate various polarization control devices. In this section, examples will be given how the novelties mentioned above are exerted for waveguide devices.

Post-Photobleaching for Device Tuning

For waveguide devices, imperfection of fabrication processing can seriously affect the device performance such as the extinction ratio of Mach-Zehnder modulators, switching extinction of directional coupler switches, and the splitting ratio of Y-junction splitters. It is therefore very valuable if one can tune the specification of the devices after the completion of the device fabrication to improve the device performance.

Photobleaching technique enables one to do it. The ides stems from the fact that many EO polymers can be bleached out upon irradiation of UV or VIS light, resulting in lowering of the refractive index[36]. If the some part of the waveguide is not perfectly fabricated as desired, the part can be trimmed to tune the specification of the device. The trimming can be executed *in situ* while monitoring the device performance. The

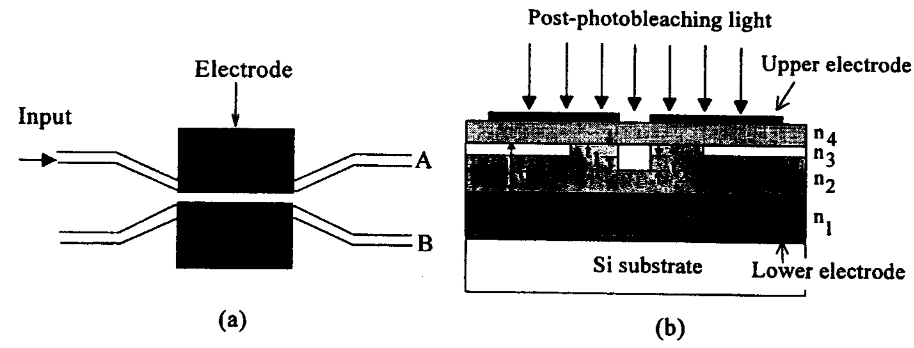

Fig. 5. Schematic diagrams of a directional coupler switch: (a) top view and (b) cross sectional view. Post photobleaching process is schematically shown in (b).

value of the technique is manifested by taking an example of the directional coupler switch[23].

The structure of the directional coupler switch is schematically shown in Fig. 5. Light coupled in one arm at one side can be switched to the bar state (A in Fig. 5(a)) or the cross state (B in Fig. 5(b)) depending on the voltage applied to the electrode on top of the waveguides. Coupling of the light can be expressed by the coupling constant of the switch. In order to have a good switching extinction in the device, the initial output state must be in the cross state. To satisfy the condition, the coupler length L should be equal to[28, 29]:

$$L = (1 + 2m)L_c = (1 + 2m)\frac{\pi}{2c} \qquad (2)$$

where m is an integer, L_C the coupling length, and c the coupling constant. The coupling constant depends on the many waveguide parameters such as the propagation constant, the damping constant, and the gap width, etc.. In real fabrication processes, it is almost impossible to control all the parameters exactly to satisfy Eq. (2). By the reason, it is valuable to find a method, which can control the coupling length or coupling constant independently with the fabrication process.

Since the coupling constant varies with the effective refractive index in the gap region of the planar waveguide, the output state can be adjusted by the selective photobleaching of the gap region after the completion of the device fabrication. By performing the photobleaching while monitoring the outputs from the two waveguides, the output state can be tuned exactly to the cross state by the method so called post-photobleaching technique.

The post-photobleaching process is schematically shown in Fig. 5(b). The patterned switching electrodes are located on both waveguide channels, so that the gap region is open to the post-photobleaching light. As the bleaching proceeds in the gap region, the refractive index of the region becomes smaller and the coupling constant becomes smaller too. Since the initial output powers of the cross (P_{cross}) and the bar (P_{bar}) states in a symmetric directional coupler can be expressed by[28]

$$P_{cross} / P_{in} = \sin^2(cL) \qquad (3)$$

$$P_{bar} / P_{in} = 1 - \sin^2(cL), \qquad (4)$$

the initial output states with no bias can be tuned by controlling the post-photobleaching depth of the gap region. Details of the mathematical description of the method has been described elsewhere[27].

For the demonstration purpose, we fabricated the directional coupler switch using P2ANS as an EO polymer[32]. The directional coupler type channel waveguide was formed by photobleaching using a mask aligner (Karl Suss MJB3). The waveguide was poled at 140 °C for 10 min with the poling field of about 2 MV/cm over the whole region including the input and output stages. Switching electrodes were formed using the poling electrode by etching process. The initial bleaching depth was 0.2 μm, which was estimated by comparing the observed mode size and the calculated one. The coupler length L is 18 mm. The waveguide width and the gap width are 4 μm and 2 μm, respectively. The completed devices were cleaved for test. 1.3 μm light from a laser diode was coupled to one arm in the input side by end fire coupling and measured the output powers from the both arms of output with a vidicon camera. Selective post-photobleaching was performed to the gap region while monitoring the output states using 458 nm light from Ar+ laser with the light intensity of 8 mW/cm^2.

Fig. 6 shows the evolution of the experimental output power from the cross and the bar states as a function of the total bleaching depth. The calculated power evolutions are also shown with the solid line and the dotted line. The initial output is almost in the cross state and the two successive cross states appear as the post-photobleaching proceeds. The result agrees with the calculated one very well, demonstrating that the proposed post-photobleaching technique can be utilized to tune the output state and the cross-over coupling order of the device as well.

The example clearly demonstrates that the post-photobleaching technique is a very valuable tool to tune the performance of the EO polymer waveguide devices after the completion of the device fabrication. It can improve device performance, reduce the cost and increase fabrication yield. Recently the technique was adopted to tune the extinction ratio of a Mach-Zehnder modulator. Focused laser light was used to accelerate the photobleaching process[30].

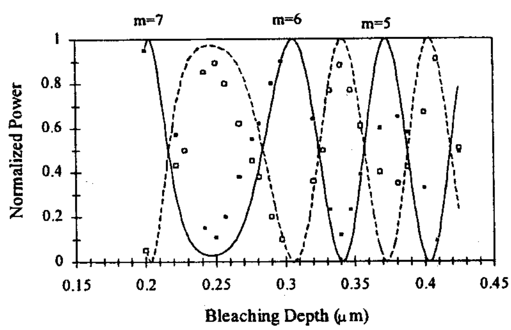

Fig. 6. The experimental output power evolutions of the cross state (■) and the bar state (□) as a function of total beach depth. The solid and dashed lines are theoretical results.

Polarization Control Devices

In EO poled polymers, the electric field-assisted poling at an elevated temperature is an essential process to induce the EO effect by breaking the centrosymmetry. The chromophores of EO polymers are aligned along the poling field direction during the poling process. As a result, the refractive index of the poled EO polymer increases for the light polarized along the poling direction (extraordinary optic axis), while it decreases for the light polarized perpendicular to the poling direction (ordinary optic axis). The refractive indices along the extraordinary and ordinary optic axes of the poled electro-optic polymers are expressed by

$$n_e = n_i + \Delta n_p \tag{5}$$

$$n_o = n_i - \frac{1}{2}\Delta n_p, \tag{6}$$

where n_i is the refractive index of the isotropic medium before poling, Δn_p the refractive index change due to the poling toward the poling direction. Δn_p is in turn related to the poling field by

$$\Delta n_p = \alpha E_p^2 , \tag{7}$$

where E_p is the local poling field and α a proportional constant.

These equations indicate that the direction of the extraordinary optic axis and the degree of the birefringence can be controlled by the direction and the magnitude of the poling electric field. Therefore, the poling process can be utilized to fabricate channel waveguides supporting single polarization component of either TE or TM modes. For instance waveguides formed by the vertical poling can confine only TM mode while TE mode radiates, which is a TM polarizer. The concept can be extended to obtain desired optic axis by poling if we design and arrange the poling electrode properly. The poling induced birefringence combined with the controllability of the optic axis can be utilized to fabricate various polarization control devices, such as polarizers[31], polarization splitters[32], polarization rotators[33,34], polarization independent modulators35, and so on. In this paper, passive and active polarization converters are briefly described.

Passive TE-TM polarization converter[33]

If the optic axis in a waveguide is made to rotate slowly along the propagation direction by a proper design of the poling electrode, the polarization of the guided mode will rotate following the gradually rotating optic axis of the waveguide as the wave propagates. This resembles the polarization rotation in the twisted nematic liquid crystal. We have utilized the concept to design and fabricate a polarization converter.

The polarization converter fabricated in this work is mainly composed of three sections: polarizer, polarization rotator, and analyzer. They are connected adiabatically. Its schematic diagram is shown in Fig. 7. Three layers stack of polymers between poling electrodes forms a planar waveguide. At the first section of the device, a polarizer is located. There are four electrodes for poling the core of the waveguide horizontally. When the poling field is applied on the electrodes with polarities as noted in the figure, the poling field direction over the core layer is mainly aligned horizontally. Because of the birefringence induced by the horizontal poling, the channel waveguide region works as a TE-pass filter.

The polarization rotator section after the polarizer has a slowly varying electrode structure which makes the optic axis rotate from horizontal to vertical direction. It is unnecessary to control the optic axis precisely in the rotator section as long as the optic axis varies slowly enough to suppress the excess scattering loss. The final section is an analyzer, which is poled by vertically aligned electrodes. Due to the birefringence induced by poling, it works as a TM pass filter.

When light is coupled into the device, a TE polarized guided mode is evolved in the polarizer section. As the light propagates along the rotator section, the polarization of the guided mode rotates from TE to TM mode following the optic axis without any inherent loss. Finally, a TM polarized guided mode comes out of the analyzer section. Because no periodic structures are included in the device, it is wavelength insensitive and its design is not critical. An analysis by vector beam propagation method for anisotropic media showed that efficient polarization conversion is possible if the rotator section is longer than 1 mm.

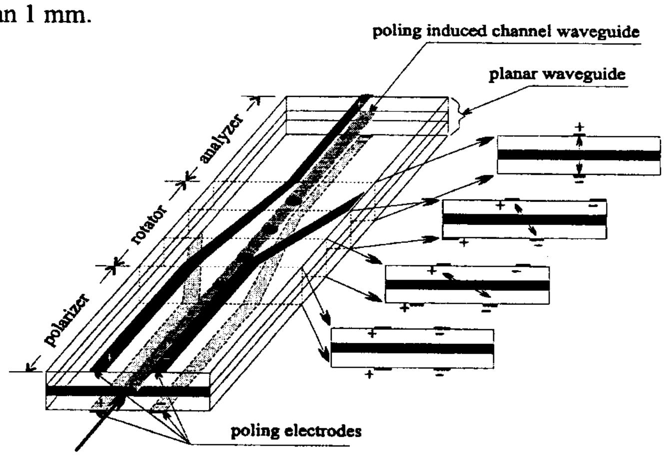

Fig. 7. Schematic diagram of the proposed polarization rotator: cut-views show the major direction of the poling field or the optic axis of the poling induced waveguide for given structure.

The device was fabricated on a thermally oxidized Si wafer. Bottom electrodes were formed by thermal evaporation of Ti-Au layer followed by lift off process. Lower cladding, guiding, and upper cladding layers were successively spin coated with the thickness of 3.5 μm, 4 μm and 2 μm, respectively. The materials of the core and lower buffer layers were electro-optically active side chain polymers with slightly different chromophore composition. Top electrodes were formed by wet etching process of thermally evaporated Au layer. Finally the device was poled followed by cleaving for test. Details of the fabrication process are reported elsewhere[31]. 1.3 μm light from a laser diode was launched to the waveguide by end fire coupling. The output light was collected with a microscope object through a Glan-Thompson polarizer. The power in each polarization component was measured by the device.

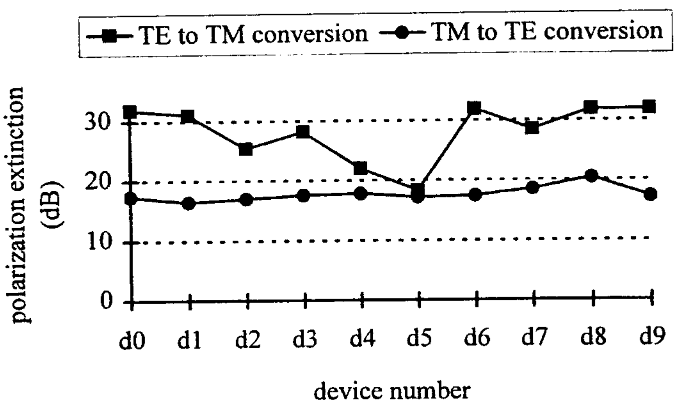

device number	d0	d1	d2	d3	d4	d5	d6	d7	d8	d9
L_T (mm)	3	3	3	3	3	4	4	4	4	4
W_g (μm)	10	8	8	6	6	6	6	8	8	10
W_e (μm)	8	8	6	6	4	4	6	6	8	8

Fig. 8. Measured polarization extinction ratio of the output light of the 10 polarization converters fabricated with different electrode parameters. It was measured for both TE to TM and TM to TE conversions.

The measured polarization extinction ratios for the TE to TM mode conversion are shown in Fig. 8 for different waveguide dimensions. In the figure, L_r is the length of the rotator section, W_g the width of the gap between the electrodes in the polarizer section, W_e the width of the electrode in the analyzer. W_e and W_g were chosen to satisfy the single mode condition of the channel waveguide. A complete TE to TM mode conversion was observed and the polarization extinction ratio of the output light was higher than 30 dB for the best device. The excess loss was smaller than 1 dB for all the devices.

The TE to TM mode conversion efficiencies were also measured by reversing the light propagation direction and the input polarization. The measured results are also shown in Fig. 8. The polarization extinction ratio higher than 20 dB was obtained. However the results are worse than the case of TE to TM mode conversion. The vertical poling electrode structure is almost ideal for TM polarization so that the quasi-TM mode of the waveguide has negligible TE component. On the other hand, the horizontal poling is less ideal than the vertical poling and supports the quasi-TE mode that retains a little TM component. This fact may cause the degradation of the output polarization extinction ratio for the TM to TE mode conversion.

Active Polarization Converter

The concept of the controllability of optic axis in poled polymers can be extended to realize an active polarization converter. The proposed active TE-TM mode converter is schematically shown in Fig. 9. The waveguide coordinate x-,y-,z- and the poling induced principal axes a-, b-, c- are shown in the figure. Light propagates along the z-direction. The core region is electro-optically active and its optic axis is inclined 45°

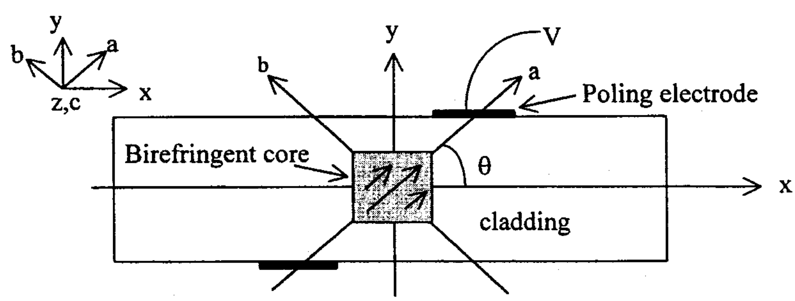

Fig. 9. Cross sectional view of the proposed mode converter with the coordinate convention. The principal axes a, b, c of the poled core has the rotational angle of θ with respect to the waveguide coordinate x, y, z. Light propagates along the z axis.

against the surface normal. The device structure can be realized by EO poled polymers, because the optic axis in the poled polymers are parallel to the poling field.

When TM or TE mode propagates through the birefringent waveguide, the polarization state of the light will vary with propagation distance because of the phase retardation between two normal modes, E_a and E_b. If the birefringent medium is electro-optically active, the polarization of the output light can be controlled by the electric field applied along the optic axis. The electrodes used for poling can be utilized as the controlling electrodes themselves.

It is not easy to get perfectly 45° off uniform optic axis over the core region in three layers stack poled polymer waveguides. However, it is possible to obtain nearly uniform poling field in the core region by adjusting the width of the poling electrodes and the lateral displacement. One example of the poling field distribution in a 20 μm thick waveguide is shown in Fig. 10, where 10 μm wide upper and lower poling electrodes were laterally separated by 14 μm (center to center). Average poling field direction in the 5 μm x 5 μm core region is 44.8° with standard deviation of 1.7°. In fact, around 5° spatial variation of the optic axis in the core region turns out not to affect the conversion efficiency of the device significantly. More complicated electrode structure may result in more uniform poling field distribution over the waveguide. The poling electrodes themselves can be utilized as the signal electrodes to modulate the core birefringence, therefore the output polarization state.

Under the above conditions, one restriction for the efficient polarization conversion from the device is the spatial profile mismatch between the normal modes due to the refractive index birefringence of the core medium. We have analyzed the restriction by the vector beam propagation method and demonstrated that the conversion efficiency over 98 % can be achieved if the poling induced birefringence is small

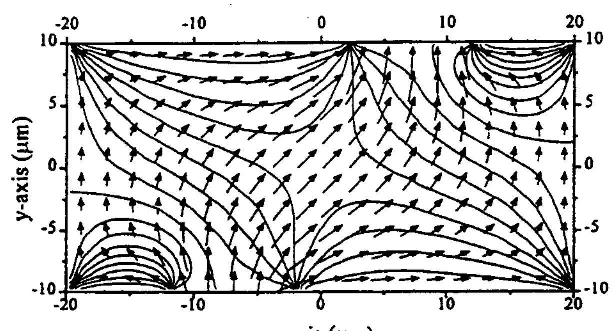

Fig. 10. Calculated poling field direction and poling angle contour for 20 μm thick film. The length of the arrow indicates the field magnitude. The electrode width and the lateral center-to-center displacement are 10 μm and 14 μm, respectively.

against the surface normal. The device structure can be realized by EO poled polymers, because the optic axis in the poled polymers are parallel to the poling field.

SUMMARY

Recent advances in electro-optic polymer waveguide devices are summarized. Very high speed electro-optic modulator has been realized recently, and some devices are under field test for practical use. Along with the modulators, novel switches and various polarization control devices have been actively pursued, resulting in high performance devices. Those devices are utilizing the unique properties of EO poled polymers such as the flexibility of the fabrication process and the controllability optic axis, which are not possible in other materials. A method to tune the specification of waveguide devices after the completion of the device fabrication is also introduced, which is called post-photobleaching technique. This is a valuable technique to increase the fabrication yield.

REFERENCES

1. D.Chen, H. R. Fetterman, A. Chen, W. H. Steier, L. R. Dalton, W. Wang, and Y. Shi, Appl. Phys. Lett. 70, 3335 (1997).
2. S. R. Marder, B. Kippelen, A. K.-Y. Jen, N. Peyghambarian, Nature 388, 845 (1997).
3. M. Ahlheim, et al., Science 271, 335 (1996).
4. M. A. Mortazavi, H. N. Yoon, and C. C. Teng, Appl. Phys. Lett. 74, 4871 (1993).
5. C. C. Teng, M. A. Mortazavi, and G. K. Boudoughian, Appl. Phys. Lett. 66, 667 (1995).
6. H. Park, W.-Y. Hwang, J.-J. Kim, Appl. Phys. Lett. 70, 2796 (1997).
7. A. Yariv, Quantum Electronics, New York, John Wiley and Sons, 1989, p322.
8. D. G. Girton, S. L. Kwiakowski, G. F. Lipscomb, and R. S. Lytel, Appl. Phys. Lett. 20, 1730 (1991).
9. C. C. Teng, Appl. Phys. Lett. 60, 1538 (1992).
10. R. S. Moshrefzadeh, K. M. White, C. V. Francis, M. W. Kleischmit, S. K. Mohapatra, G. T. Boyd, R. C. Williams, K. H. Hahn and D. W. Dolfi, OSA Tech. Dig. Ser., Washington DC: Op. Soc. Amer. Vol. 17, 325 (1993).
11. W. Wang, D. Chen, H. R. Fetterman, Y. Shi, W. H. Steier, and L. R. Dalton, IEEE Photon. Technol. Lett. 7, 638 (1995).
12. Y. Shuto, S. Tomaru, M. Hikita, and M. Amano, IEEE Quantum Electron. 31, 1451 (1995).
13. S. Ermer, W. W. Anderson, T. E. VanEck, D. G. Girton, J. A. Marley, A. Harwit, S.

M. Lovejoy, and D. S. Leung, Organic Thin Films for Photonic Applications, OSA Tech. Dig. , Washington DC: Opt. Soc. Amer. 21, 285 (1995)

14. W. Wang, D. Chen, H. R. Fetterman, Y. Shi, W. H. Steier, and L. R. Dalton and P. D. Chow, Appl. Phys. Lett. 67, 1806 (1995).
15. Y. Shi, W. Wang, J. H. Bechtel, A. Chen, S. Garner, S. Kalluri, W. H. Steier, D. Chen, H. R. Fetterman, L. R. Dalton, and L. Yu, IEEE J. Selected Topics in Quantum Electron. 2, 289 (1996).
16. M. H. Lee, H. J. Lee, S. G. Han, H.-Y. Kim, K. H. Kim, Y. H. Won, S. Y. Kang, Thin Solids Films 303, 287-291 (1997).
17. J.-J. Kim, W.-Y. Hwang and T. Zyung, Mol. Cryst. Liq. Cryst. 267, 353 (1995).
18. J.-J. Kim and W.-Y. Hwang, Mol. Cryst. Liq. Cryst. 15, 307 (1996).
19. W.-Y. Hwang and J.-J. Kim, Appl. Phys. Lett. 69 (11), 1520 (1996).
20. H.-M. Lee, W.-Y. Hwang, M.-C. Oh, H. Park, T. Zyung, J.-J. Kim, Appl. Phys. Lett. 71, 3779 (1997).
21. Y. Shi, W. Wang, W. Lin, D. J. Olson, J. H. Bechtel, Appl. Phys. Lett. 71, 2236 (1997)
22. E. Van Tomme, P. Van Daele, R. Bates, G. R. Mohlmann, and M. B. J. Dimmeer, J. Appl. Phys. 69, 763 (1995)
23. W.-Y. Hwang, J.-J. Kim, T. Zyung, M.-C. Oh and S.-Y. Shin, Appl. Phys. Lett. 67, 763 (1995).
24. J. I. Thackara, J. C. Chon, G. C. Borklund, W. Volksen, and M. Burland, Appl. Phys. Lett. 67, 3874 (1995).
25. W.-Y. Hwang, M.-C. Oh, H.-M. Lee, H. Park, and J.-J. Kim, IEEE Photon. Technol. Lett. 9, (1997 (1997).
26. W. K. Burns and F. Milton, IEEE J. Quantum Electron. QE-16, 446 (1980).
27. H. Feng, X-Li, Z. Yang, and M. Wang, Appl. Phys. Lett. 60, 2843 (1980).
28. A. Yariv and P. Yeh, Optical Waves in Crystals, John Wily & Sons, New York (1984), pp459-469
29. R. V. Schmidt and R. C. Alferness, IEEE Trans. Circuits Syst., **CAS-26**, 1099 (1979)
30. A. Chen, F. I. Marti-Carrera, V. Chuyanov, S. Garner, W. H. Steier, S. S. H. Mao, Y. Ra, L. R. Dalton, Y. Shi, Organic Thin Films for Photonics Applications, OSA Technical Digest Series 14, 211 (1997)
31. M.-C. Oh, S.-Y. Shin, W.-Y. Hwang and J.-J. Kim, IEEE Photonics Technol. Lett. 8, 375 (1996).
32. M.-C. Oh, S.-Y. Shin, W.-Y. Hwang and J.-J. Kim, IEE Electron. Lett. 32, 324 (1996).

33. M.-C. Oh, S.-Y. Shin, W.-Y. Hwang and J.-J. Kim, Appl. Phys. Lett. 67 (13), 1821 (1995).
34. W.-Y. Hwang, J.-J. Kim, T. Zyung, M.-C. Oh and S.Y. Shin, IEEE J. Quantum Electron. 32, 1054 (1996).
35. M.-C. Oh, W.-Y. Hwang, H. J. Lee, M. H. Lee, J.-H. Ahn, H. Park, S. G. Han, and Y.-H. Won, Organic Thin Films for Photonics Applications, OSA Technical Digest Series 14, 188 (1997)
36. J.-J. Kim, T. Zyung and W-Y Hwang, Appl. Phys. Lett. 64, 3488-3490 (1994).

This paper will be published in "Nonlinear Optics"